THE JOURNAL OF BIOLOGICAL CHEMISTRY VOL. 290, NO. 26, pp. 16142–16156, June 26, 2015

Extended Synaptotagmin Interaction with the Fibroblast Growth Factor Receptor Depends on Receptor Conformation, Not Catalytic Activity*

Received for publication, April 5, 2015, and in revised form, April 24, 2015 Published, JBC Papers in Press, April 28, 2015, DOI 10.1074/jbc.M115.656918

Michel G. Tremblay, Chelsea Herdman, François Guillou, Prakash K. Mishra, Joëlle Baril, Sabrina Bellenfant, and Tom Moss[1]

From the Laboratory of Growth and Development, St-Patrick Research Group in Basic Oncology, Cancer Division of the Québec University Hospital Research Centre, and Department of Molecular Biology, Medical Biochemistry and Pathology, Faculty of Medicine, Laval University, Edifice St Patrick, 9 rue McMahon, Québec, Québec G1R 3S3, Canada

Background: Extended Synaptotagmins selectively bind the active FGF receptor but the mechanism is unknown.
Results: ESyt2 and 3 but not ESyt1 recognize the active conformation of the FGF receptor independently of catalytic activity.
Conclusion: ESyt2 and probably ESyt3 access the active cleft of the FGFR1 kinase domain.
Significance: How ESyts recognize FGFRs is essential to understanding how they modulate receptor signaling.

We previously demonstrated that ESyt2 interacts specifically with the activated FGF receptor and is required for a rapid phase of receptor internalization and for functional signaling via the ERK pathway in early *Xenopus* embryos. ESyt2 is one of the three-member family of Extended Synaptotagmins that were recently shown to be implicated in the formation of endoplasmic reticulum (ER)-plasma membrane (PM) junctions and in the Ca^{2+} dependent regulation of these junctions. Here we show that ESyt2 is directed to the ER by its putative transmembrane domain, that the ESyts hetero- and homodimerize, and that ESyt2 homodimerization *in vivo* requires a TM adjacent sequence but not the SMP domain. ESyt2 and ESyt3, but not ESyt1, selectively interact *in vivo* with activated FGFR1. In the case of ESyt2, this interaction requires a short TM adjacent sequence and is independent of receptor autophosphorylation, but dependent on receptor conformation. The data show that ESyt2 recognizes a site in the upper kinase lobe of FGFR1 that is revealed by displacement of the kinase domain activation loop during receptor activation.

The Extended Synaptotagmin-like proteins (ESyts)[2] are similar in general structure to the Synaptotagmins, a C2 domain-containing family of proteins involved in calcium-mediated secretion and endocytosis (1). So far three proteins have been discovered that belong to the Extended Synaptotagmin family, ESyt1, ESyt2, and ESyt3. ESyt1 was originally discovered in vesicle preparations from rat adipocytes and named vp115 for 115kDa vesicular protein (2). However, it was not until 2007 that all three family members were initially studied and the name Extended Synaptotagmin first coined (3). The domain architecture of the human ESyts revealed a putative N-terminal transmembrane domain (TM), an SMP (Synaptotagmin-like Mitochondrial lipid-Binding Protein) domain (4) followed C-terminally by multiple C2 domains. Human ESyt2 and ESyt3 each contain three C2 domains (C2A, C2B, and C2C) while ESyt1 has five (C2A to C2E) (Fig. 1*A*), and this organization is conserved in mouse (5), *Xenopus* (6) and to a surprising extent in the yeast Tricalbins (7).

Jean *et al.* (6) provided the first potential function for ESyt2 when they showed that it acted as an endocytic adapter specific for the activated FGF receptor and was required for functional signaling via the ERK MAP-kinase pathway during early *Xenopus* development. *Xenopus* ESyt2 was also later shown to recruit the p21-GTPase Activated Kinase PAK1 and to regulate the dynamics of the actin cytoskeleton (8). More recently, the yeast Tricalbins were shown to be endoplasmic reticulum (ER)-resident proteins that aid in the formation of ER to plasma membrane junction sites or bridges (9), and the human ESyts were shown to play a similar role (10, 11). The ESyts were also shown to associate with the ER membrane, probably via a TM hairpin, and to help tether the ER to the PM. Further, ESyt1 was shown to respond to cytosolic Ca^{2+} by translocating to the sites of ER-PM junctioning and to promote the replenishment of PM-associated phosphatidylinositol 4,5-bisphosphate (PIP2) (10).

Here we have investigated the molecular basis for the specificity of the ESyt-FGFR interaction. We have characterized the homologous and heterologous interactions between the human ESyts, the interactions of each with FGFR1, defined the homologous interaction and ER targeting domains of ESyt2 and used extensive deletion and point mutations to

* This work was supported by a Cancer Research Society (CRS/SRC) grant (to T. M.). The Quebec University Hospital Research Centre (CR-CHU de Québec) is supported by a grant from the FRSQ (Québec). The authors declare that they have no conflicts of interest with the contents of this article.
[1] To whom correspondence should be addressed: Laboratory of Growth and Development, St-Patrick Research Group in Basic Oncology, Cancer Division of the Québec University Hospital Research Centre, Edifice St Patrick, 9 rue McMahon, Québec, QC G1R 3S3, Canada. Tel.: 1-418-691-5281; Fax: 1-418-691-5439; E-mail: Tom.Moss@crhdq.ulaval.ca.
[2] The abbreviations used are: ESyt, Extended Synaptotagmin; FGF, fibroblast growth factor; FGFR, fibroblast growth factor receptor; PIP, phosphatidylinositol 4,5-bisphosphate; SMP, synaptotagmin-like mitochondrial lipid-binding protein; TM, transmembrane domain; ER, endoplasmic reticulum: PM, plasma membrane; PEI, polyethylenimine; PLCγ, phospholipase Cγ; AMP-PCP, β,γ-methyleneadenosine 5′-triphosphate; aa, amino acid.

investigate the molecular specificity of the ESyt2-FGFR1 interaction. The data surprisingly reveal a mode of interaction that is independent of receptor autophosphorylation, or indeed catalytic activity, and is solely dependent on the active receptor conformation. The data show that ESyt2 recognizes a site in the upper kinase lobe of FGFR1 that is revealed when the activation loop is displaced into the active configuration.

Experimental Procedures

Plasmid Constructs—Full-length human ESyt1, ESyt3, and Syt1 cDNAs were amplified from total MCF-7 cDNA and corresponded in coding sequence to FAM62A (NM_015292), FAM2C (NM_031913), and SYT1 (NM_005639). Construction of the human ESyt2b splice variant cDNA was previously described (6) and was equivalent in reading frame sequence to FAM62B (NM_020728). The open reading frame for the human ESyt2a splice variant was created from the ESyt2b cDNA by replacing the sequences 5′ of the unique SacII site with a synthetic custom gene fragment (Integrated DNA Technologies, IDT) corresponding to the equivalent region of sequence DQ993201. All the ESyt mutants and epitope-tagged constructs were created in these original cDNAs, subcloned in PCDNA3, and the full coding sequence of each was determined. The human FGFR1 was obtained from J. Wesche and E. M. Haugsten and was subcloned along with a FLAG N- or HA C-terminal epitope tag in the pCS2+ vector. FGFR1 mutants were created directly in these constructs using the QuickChange strategy (Agilent Technologies) or by direct PCR amplification and the full coding sequence of each final mutant was determined.

Cell Culture and Transfections—HEK293T cells were cultured in Dulbecco's Modified Eagle's Medium supplemented with 10% fetal bovine serum (Wisent). 1.25×10^6 293T cells were seeded on poly-L-lysine (1 mg/ml) (Sigma) treated 60-mm Petri dishes 24 h prior to transfection. Transfections were performed using branched polyethylenimine (PEI) (Sigma 408727) (12–14). Briefly, DNA (~5 μg, amount varied dependent on expression vector) was diluted in 400 μl of Opti-MEM medium (Invitrogen) followed by the addition of PEI at 2 mg/ml to obtain a 1:2 ratio). The solution was then vortexed for 10 s and left at room temperature for 5 min, before adding dropwise to the cells. Where indicated, cells were treated with 25 μM SU-5402 (Symansis Cell Signaling Science) or with bFGF (Sigma), 20 ng/ml, and heparin (Sigma), 5 μg/ml.

Coimmunoprecipitation—HEK293T cells were processed for co-immunoprecipitation as previously described (6). Briefly, 20 μg of anti-HA (12CA5) and 20 μl of a slurry of Protein A-Sepharose (GE Healthcare), or 20 μl of anti-FLAG agarose beads (Sigma), prepared following manufacturer's instructions was added to the lysates and incubated at 4 °C for 2 h. Bound proteins were eluted with 2× SDS-PAGE loading buffer, fractionated on Tris-glycine SDS-PAGE gels, transferred to nitrocellulose membrane (Bio-Rad) and probed with the appropriate antibody. For Western blotting, antibodies were used at 1/1000 (anti-HA, Abcam), 1/1000 (anti-Myc, Cell Signaling), 1/400 (anti-FLAG, Sigma), 1/1000 (anti-Phospho-Tyr783-PLCγ, Cell Signaling), 1/1000 (anti-PLCγ, Abcam), 1/5000 (anti-Phospho-Tyr (PY99), Santa-Cruz Biotechnology), and 1/250 (anti-ESyt2, Sigma).

Immunofluorescence Imaging—Cells were washed with PBS, fixed in 4% PFA for 15 min, and permeabilized with 0.5% Triton in PBS for 5 min. Incubation with the appropriate primary antibodies was performed for 1 h in PBS, 5% BSA, or goat serum, and cells were then stained with AlexaFluor 488, 568, or 647-conjugated anti-rabbit or mouse secondary antibodies (Molecular Probes) and counterstained with DAPI. After mounting in 50% glycerol, 50% glycine buffer (0.2 M Na-glycine, 0.3 M NaCl), three-dimensional epifluorescent image stacks were acquired using a Leica SP5 II confocal microscope, equipped with a 63× immersion objective, running in standard scanning.

For FGFR1 uptake assays the above protocol was modified as follows; cells expressing N-terminally FLAG-tagged FGFR1 and HA-tagged ESyt2b were rinsed in Opti-MEM (Invitrogen) and then incubated for 1 h at 4 °C with rabbit anti-FLAG antibody diluted 1/500 in Opti-MEM. Subsequently cells were rinsed twice in Opti-MEM at 4 °C, incubated for 20 min in Opti-MEM-containing bFGF (Sigma), 20 ng/ml, and heparin (Sigma), 5 μg/ml at either 37 °C or 4 °C (control), rinsed twice, and stained "live" with AlexaFluor 568-conjugated anti-rabbit antibody diluted 1/250 in Opti-MEM for 1 h at 4 °C. Cells were then fixed and permeabilized before incubation with mouse anti-HA antibody (12CA5) and staining with AlexaFluor 488-conjugated anti-rabbit and AlexaFluor 647-conjugated anti-mouse antibodies, and counterstaining with DAPI.

The use of SNAP-tags (New England Bioloabs) followed the manufacturer's recommendations. Briefly, cells were incubated for 30 min in cell impermeable SNAP-Surface AlexaFluor 488 in culture medium. After three rinses in culture medium, cells were further incubated for 30 min in cell permeable SNAP-Cell TMR-Star in culture medium. Cells were rinsed three times over 30 min to permit unreacted SNAP-Cell ligand to diffuse out of cells, then fixed, and observed as above.

In Vitro Pull-down Assay—Combined *in vitro* transcription/translation of WT and mutant FLAG-hESyt2b proteins (cloned in pCDNA3) were carried out using the T7-TNT transcription-translation kit (Promega) using unlabeled and ^{35}S-labeled methionine. The reaction mixture was diluted to 1 ml with Nonidet P-40 lysis buffer (25 mM Tris-HCl, pH 8, 50 mM NaCl, 1% Nonidet P40). A 250-μl aliquot was used for each pull-down assay. Equal amounts of bacterially expressed GST, GST-FGFR1 aa361–752, GST-FGFR1 aa361–562, and GST-FGFR1 aa361–550 were immobilized on G-Sepharose (GE Healthcare) and incubated with *in vitro*-translated E-Syt2 WT or ΔTM for 2 h at 4 °C. The G-Sepharose was then washed five times with Nonidet P-40 lysis buffer and eluted proteins resolved on SDS-PAGE. After electrophoretic transfer the proteins were revealed by Ponceau Red staining followed by Western blot using FLAG-HRP antibody (Sigma) or, in the case of ^{35}S labeling, by phosphoimaging on a FLA-5100 (FUJIFILM Life Science).

Results

Given the general structural similarity to the synaptotagmins, the ESyts were originally assumed to be plasma membrane (PM) proteins (Fig. 1, *A* and *E*) (3, 6). However, at the time

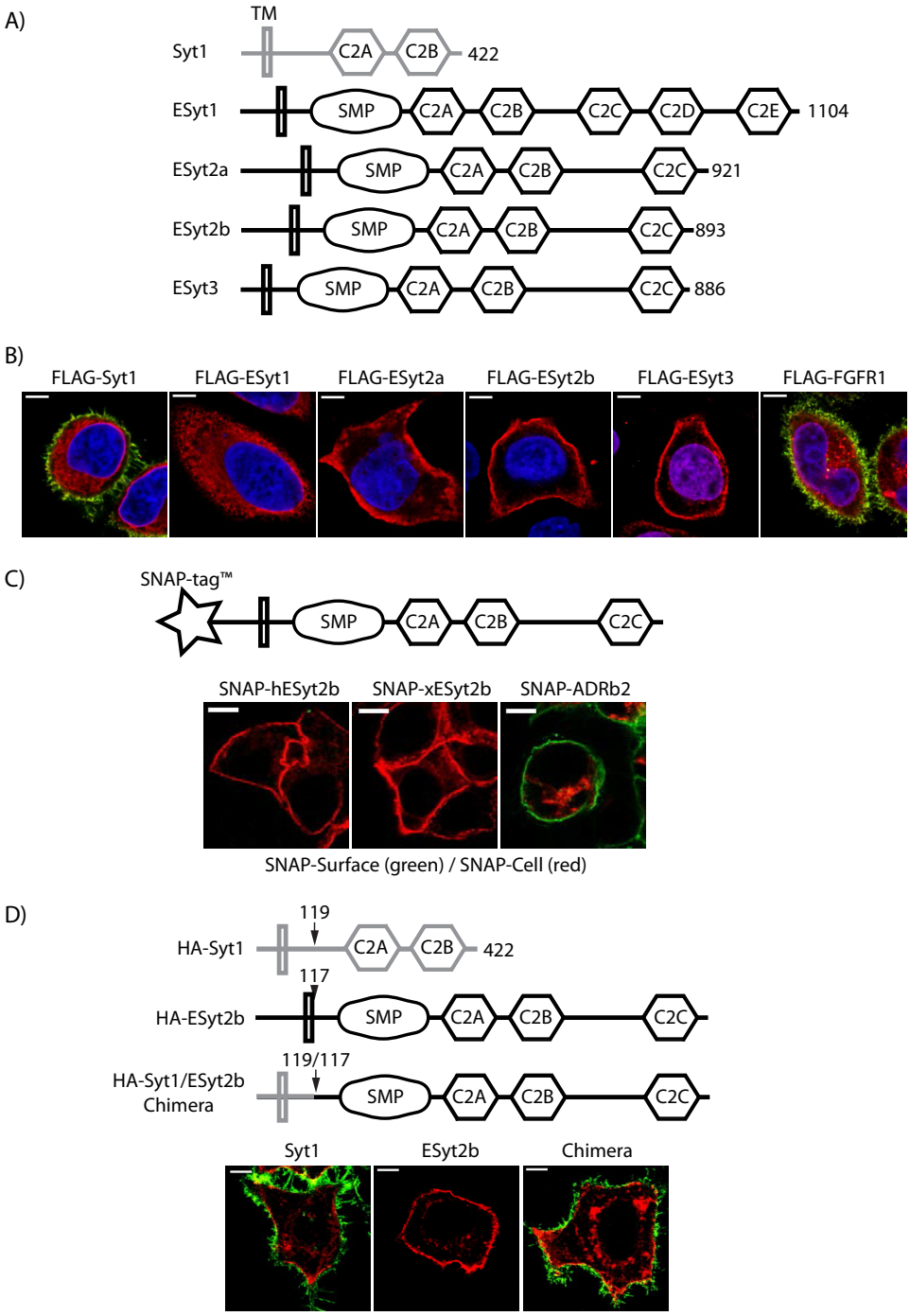

FIGURE 1. **ESyt1, -2, and -3 do not penetrate the plasma membrane.** *A*, diagrammatic structure of the human ESyt family members, including the two studied splice variants of ESyt2, in comparison with human Syt1. *B*, sequential anti-FLAG immunofluorescence (*IF*) labeling of N-terminally FLAG-tagged Syt1, ESyt1, -2, and -3 and the human FGFR1 receptor. The tagged proteins were transiently expressed in HEK293T cells and then labeled before (*green*) and after (*red*) membrane permeabilization. *C*, N-terminally SNAP™-tagged human and *Xenopus* ESyt2, and the adrenergic receptor b2 (ADRb2) were expressed in HEK293T and labeled using the SNAP-Surface and SNAP-Cell ligands following the manufacturer's instructions (New England Biolabs). *D*, N-terminally HA-tagged Syt1, ESyt2b, and Syt1/ESyt2b fusion proteins were expressed and subjected to anti-HA IF labeling before (*green*) and after (*red*) cell permeabilization as in *B*. The scale bar in *B* to *D* indicates 6 μm. *E*, alignment of the predicted amino acid sequences of the human ESyts 1, 2a, 2b, and 3 (Acc. No. NP_056107, ABJ97706.1, NP_065779.1, and NP_114119.2. The putative transmembrane domains are shown in *red*, the SMP domain in *green* and the C2 domains in *yellow*, *cyan*, *magenta*, *orange* and *blue*.

we were unable to detect these proteins on the PM via N-terminal FLAG epitope-tags (Fig. 1*B*), or indeed HA-tags (data not shown) despite the same tags being fully available after cell permeabilization. A SNAP-tag™ fused to the N terminus of ESyt2b was also not available before cell permeabilization, despite an N-terminal SNAP-tag fused to the adrenergic receptor b2 (ADRb2) being easily detected with both the cell-impermeable SNAP-surface and cell permeable SNAP-Cell ligands (NEB) (Fig. 1*C*). Recently it was found that rather than being inserted into the PM the ESyts are probably inserted into the membrane of the endoplasmic reticulum (ER) (10, 11). These data exclude the possibility that the ESyts traverse the PM and are consistent

E)

FIGURE 1—*Continued*

with an association with the ER, but also with a non-penetrating mode of membrane association such as recently proposed (10, 11).

ESyt2b Is Misdirected to the PM by Fusion to the Syt1 Transmembrane (TM) Domain—Exactly what directs the ESyts to insert exclusively into the ER membrane rather than into the PM as does Syt1 is presently not known. To resolve this question we created a fusion between Syt1 and ESyt2b, such that the potential transmembrane/membrane-insertion (TM) domain and N-terminal sequences of ESyt2b were replaced by those of Syt1. This resulted in an ESyt that associated with and penetrated the PM much as did Syt1 (Fig. 1*D*). Given that the ESyts and their splice variants display little if any homology preceding the potential membrane-associated domain (Fig. 1*E*), this strongly suggests that the determinants for association with the ER membrane lie within the membrane-associated domain or the ~20 aa preceding it.

The ESyts Homo- and Hetero-dimerize—Given their localization in the ER, to better understand the function of the ESyts in FGF signaling, we first wished to establish if they function as monomers or as hetero- or homodimers. Recent data demonstrated that the ESyts can probably heterodimerize and homodimerize (6, 11). Consistent with this, when differentially tagged versions of the three ESyts were expressed in homologous and heterologous pairs, it was evident that not only did all three heterodimerize, but also homodimerize (Fig. 2). ESyt1 interacted with itself, with the two N-terminal splice forms of

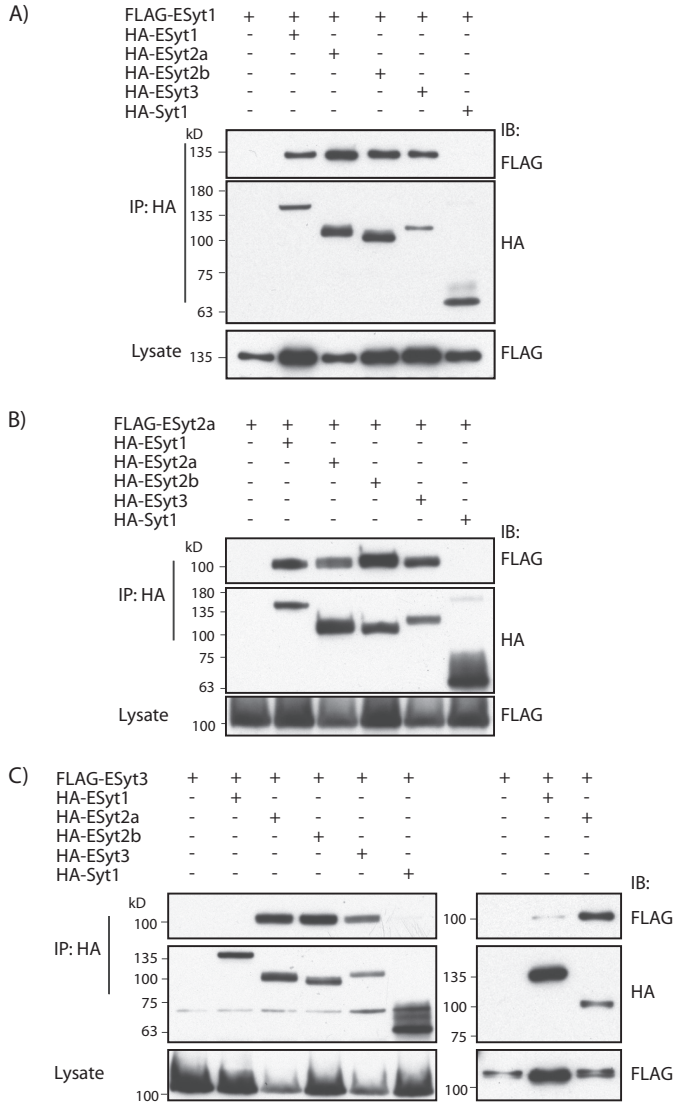

FIGURE 2. **All three ESyt proteins and splice variants homo- and heterodimerize *in vivo*.** *A*, N-terminally FLAG-tagged human ESyt1 was co-expressed in HEK293T cells with each of the other N-terminally HA-tagged human ESyt forms and human Syt1. Subsequently, co-immunoprecipitation of FLAG-tagged ESyt1 was determined by Western blot. *B* and *C*, same analysis was performed respectively for N-terminally FLAG-tagged ESyt2a and ESyt3.

ESyt2, (2a and 2b, Ref. 6) (Fig. 2*A*), and with ESyt3. ESyt2a interacted both with itself and its N-terminal splice variant ESyt2b, as well as with ESyt1 and 3 (Fig. 2*B*), and conversely ESyt3 interacted with both ESyt2a and 2b (Fig. 2*C*). ESyt3 co-expression with ESyt1 was consistently poor but clearly showed an interaction (compare Fig. 2, *C* and *A*). Since none of the three ESyts interacted with Syt1, clearly these interactions were highly specific.

ESyt2 Dimerization Maps to Its N-terminal Sequences and Does Not Require the SMP Domain—We further investigated the domain of ESyt2 responsible for its dimerization. The N-terminal regions preceding the membrane domain of ESyt2a and 2b bear little homology, suggesting that these regions were probably not involved. However, when increasingly extensive C-terminal deletion mutants of FLAG-tagged ESyt2b were co-expressed with full-length HA-tagged ESyt2b, interactions were observed with deletions mutants aa 1 to 785, lacking C2C domain, aa1 to 510 lacking C2B and C2C, aa 1 to 359 lacking all three C2 domains, and even aa 1 to 139, lacking the SMP domain (Fig. 3). Thus, the minimal homo-dimerization/oligomerization domain mapped between aa 1 and 139. This was somewhat surprising in the context of the recent crystal structure of two SMP domains that showed β-barrel structures contacting end-to-end to form a dimer (15). The data then suggest that either ESyt2 contains two or more redundant dimerization domains or that it predominantly dimerizes via sequences close to or within its putative transmembrane domain that were not present in the ESyt2 structure determination.

ESyt2 and -3, but Not ESyt1 Interact Selectively with the Activated FGF Receptor—We had previously shown that both *Xenopus* and human ESyt2 interact in a highly selective manner with the activated forms of the FGF receptor family (FGFR1–4) (6). We also showed that endogenous human ESyt2 interacts with endogenous FGFR1 in HEK293T cells, but due to a lack of adequate antibodies to either ESyt2 or FGFR1 we were unable to determine whether this endogenous interaction responded to FGF stimulation (6). We now show that this is indeed the case (Fig. 4*A*). Endogenous ESyt2 from HEK293T cells coimmunoprecipitated with exogenous FLAG-FGFR1 after FGF stimulation, and this interaction was significantly suppressed when cells were treated with the FGFR1 inhibitor SU5402. Extending these observations we found that this was a common property of the shorter two ESyts, the splice variants ESyt2a and -b and ESyt3 all displaying a strong selectivity for activated FGFR1 and little or no interaction when the receptor was specifically inhibited using SU5402 (Fig. 4, *B* and *C*). By contrast, ESyt1 repeatedly displayed little or no interaction with FGFR1 in co-transfection assays as compared with ESyt2a (Fig. 4*D*) or indeed ESyt2b or -3 (data not shown). At first sight this suggests a functional difference to the shorter ESyts. However, ESyt1 is predominantly associated with the cytosolic ER membrane and not with ER-PM junctions (Fig. 1*B*) (10, 11). Hence, the lack of interaction with FGFR may in part be a function of its different subcellular distribution.

ESyt2 May Transiently Accompany Activated FGFR during Early Endocytosis—The lack of an interaction of ESyt1 with the FGF receptor suggested that the interactions of the ESyts were at least in part determined by their subcellular distribution. We had previously shown that ESyt2 was implicated in determining receptor endocytosis and that it associates with Adaptin2 (AP-2) (6). This suggested that, consistent with its PM proximal distribution, its interaction with the activated FGF receptor initially occurs on the PM during the formation of clathrin-coated pits. We therefore asked if ESyt2b was also internalized along with activated FGFR or if its interaction was limited to the PM-associated receptor fraction. When cells expressing N-terminally FLAG-tagged FGFR1 were subjected to FGF stimulation for 20 min at 37 °C, as expected a significant level of initially PM-associated FGFR1 was observed to move into endocytic vesicles, while this internalization was prevented at 4 °C (Fig. 4*E*). In contrast, the distribution of ESyt2b (magenta) appeared to remain predominantly proximal to the PM and was not detected in FGFR1-positive endocytic vesicles (green). Further, ESyt2b did not significantly associate with early EEA1- or Rab5-

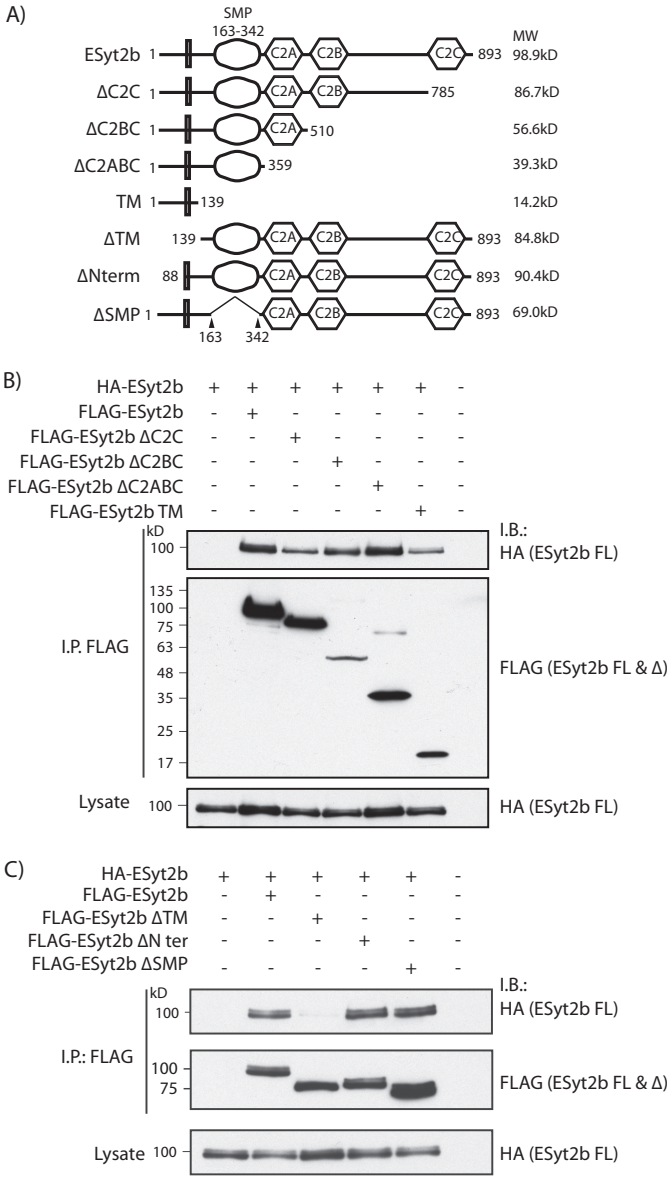

FIGURE 3. **Neither the C2 domains nor the SMP domain are essential for ESyt2b dimerization *in vivo*.** *A*, diagrammatic structure of ESyt2b and corresponding deletion mutants. *B* and *C*, analysis of co-immunoprecipitation of N-terminally HA-tagged full-length ESyt2b with the corresponding N-terminally FLAG-tagged deletion mutants co-expressed in HEK293T cells.

positive endosomes or indeed with late Rab7-positive endosomes during FGFR1 endocyosis (Fig. 4*F*). This suggested that ESyt2b interacted exclusively with the activated PM-associated FGFR1. However, it was possible that ESyt2b was internalized with FGFR1 but rapidly stripped from early vesicles, as is the case for AP-2 and clathrin. In fact, this appeared to be the case since ESyt2b immunoprecipitated with endosomes tagged with FYVE domain of the early endosomal marker EEA1 (Fig. 4*G*). This association was, however, only significant 5 min after FGF stimulation and was lost 15 min later. Thus, it is likely that ESyt2b is initially internalized with activated FGFR1, but is rapidly stripped from the early endosomes.

Interaction of ESyt2 with FGFR1 Is Mediated by a TM Adjacent Domain—To determine the structural determinants of the ESyt-FGFR interaction we used ESyt2b as a canonical model and investigated the interaction of truncation mutants with FGFR1. Co-transfection of FGFR1 with the series of ESyt2b C-terminal deletion mutants showed that loss of one, two or all of the C2 domains (ΔC2ABC) had no inhibitory effect on the interaction with FGFR1 (Fig. 5, *A* and *B*). However, deletion of the N-terminal, TM and adjacent sequences to aa136 (ΔTM) very strongly suppressed or eliminated the interaction (Fig. 5, *B* and *C*). Given that the sequences N-terminal of the TM show little or no homology between ESyt2a, 2b and 3 (Fig. 1*E*), it was not surprising that their deletion from ESyt2b (aa 1 to 87, ΔNterm) did not eliminate the interaction with FGFR1. This interaction was clearly much weaker than for the WT, though significantly greater than for the ΔTM mutation, at least in part because the ΔNterm mutant repeatedly expressed poorly (Fig. 5*B*). Specific deletion of the SMP domain had no discernable effect on the interaction with FGFR1, and the interaction was suppressed by receptor inactivation (Fig. 5*C*). Thus, the data show that the C2 and SMP domains of ESyt2b are not required for the interaction of ESyt2b with FGFR1. By contrast, this interaction does require the TM and sequences immediately flanking it (aa 88 to 138), though probably not the unconserved sequences further N-terminal (Fig. 5*D*). Hence, the domain required for ESyt2 dimerization (Fig. 3) and its interaction with FGFR1 in greater part overlap.

Interaction of ESyt2 with Activated FGFR1 Is Independent of Receptor Phosphorylation—Interactions of signaling modules with activated tyrosine kinase receptors are often mediated by receptor autophosphorylation (16). To determine if this was the case for the ESyt-FGFR interaction we generated mutations of all seven phosphotyrosine sites on FGFR1 and determined if these affected the interaction with ESyt2b. Phosphorylation of the activation loop sites Tyr-653 and -654 (Fig. 6*A*) is known to be required for FGFR1 activation (17). Consistent with this, Y to F mutation of these sites reduced receptor autophosphorylation and the interaction with ESyt2b. Further, their combined mutation (Y653,654F) suppressed both receptor autophosphorylation and the ESyt2b interaction to the same degree as the kinase dead (KD) ATP-binding site mutation K514A (Fig. 6, *A* and *B*). Thus, either ESyt2b recognized receptor phosphorylation or was able to detect the structural changes that accompany FGFR1 activation.

Individual mutation of the five non-regulatory phosphotyrosine sites (Y463, 583, 584, 730, and 766F) on FGFR1 had little if any effect on its interaction with ESyt2b (data not shown). Combined mutation of all five sites (Y5F) somewhat reduced interaction with ESyt2b, but to a much smaller extent than the activation loop mutations (Y653,654F) or the combined mutation of all 7 phosphotyrosines (Y7F) (Fig. 6*C*). Thus, interaction of ESyt2b with FGFR1 was not mediated by any single phosphotyrosine and even combined mutation of the 5 non-regulatory sites had only moderate inhibitory effects on the interaction. This left the possibility that a specific interaction with the activation loop phosphotyrosines was involved. To test this we argued that replacement of the activation loop phospho-sites of FGFR1 by phosphomimics (Y653,654E) would prevent their phosphorylation and potentially generate a constitutively activated receptor. The Y653,654E mutant displayed catalytic activity, as demonstrated by receptor autophosphoryla-

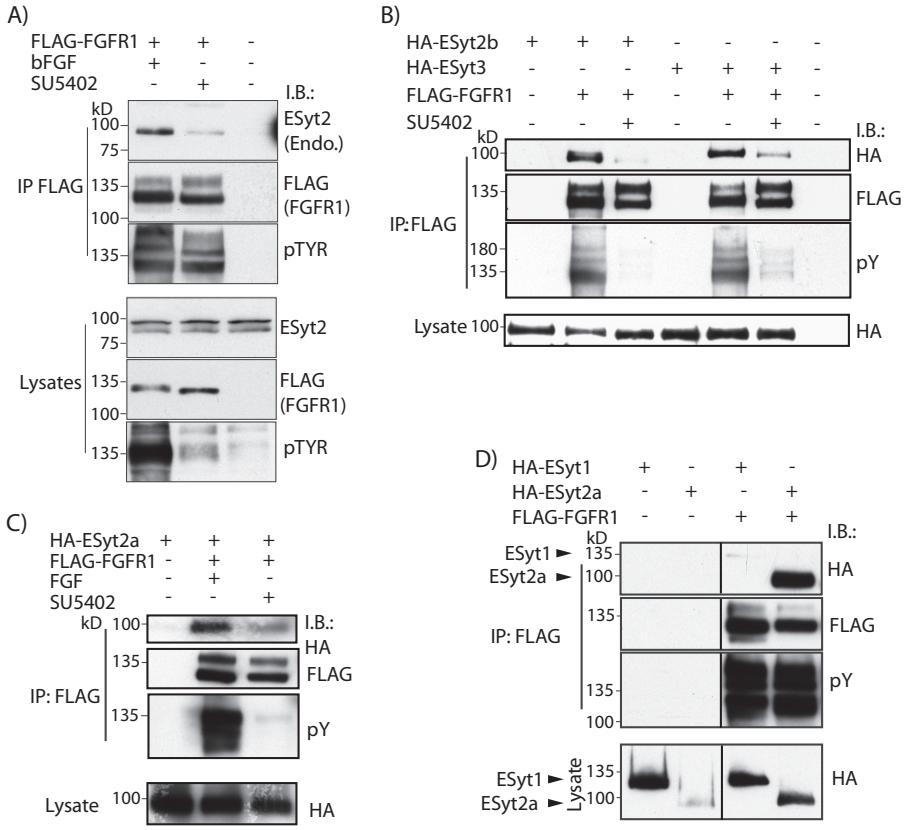

FIGURE 4. **ESyt2 and -3, but not significantly ESyt1, interact selectively with activated FGFR1.** *A*, endogenous ESyt2 is immunoprecipitated selectively with activated FGFR1. FLAG-FGFR1 was expressed in HEK 293T cells, and the receptor activated with bFGF or inhibited with SU5402 before cell lysis and immunoprecipitation of FLAG-FGFR1. *B–D*, co-immunoprecitation of N-terminally FLAG-tagged FGFR1, respectively, with N-terminally HA-tagged ESyt2b and -3, ESyt2a, and ESyt1 co-expressed in HEK293T cells after receptor activation with bFGF or inhibition with SU5402. FGFR1 activation was monitored by tyrosine autophosphorylation (*pY*). *E*, ESyt2b does not associate with FGFR1 in discrete early endosomes on stimulation with FGF. FLAG-FGFR1 and HA-ESyt2b were coexpressed in HEK293T cells, and PM-associated FGFR1 was labeled in live cell with a primary anti-FLAG antibody. After FGF stimulation (20 min) cells were labeled before fixation and permeabilization with an Alexa568-conjugated secondary (FGFR1 pre-permeabilization, *red*) then after fixation and permeabilization with an Alexa488-conjugated secondary (FGFR1 post-permeabilization, *green*) and with an HA primary, Alexa647 secondary to display HA-ESyt2b (*magenta*). The merged panels show that overlap of ESyt2b and FGFR1 (indicated by *white*) is limited to the PM (*white arrows*) and does not occur in discrete FGFR1-positive endosomes (*yellow arrows*). *F*, cells were treated as in *E* but after FGF stimulation (20 min, 37 °C) they were fixed and permeabilized, and the internalized FGFR1 (*green*) revealed in parallel with total ESyt2b (*magenta*) and the endocytic marker proteins EEA1, Rab5, or Rab7 (*red*). Newly endocytosed FGFR1 colocalizes with EEA1- and Rab5-positive, but not late Rab7-positive endosomes (*yellow*). ESyt2b displays no colocalization with either marker in cytosolic endosomes (*arrows*). *G*, ESyt2b briefly associates with early endosomes 5 min after stimulation stimulation of cells with FGF. The *upper panel* shows coimmunoprecipitation of ESyt2b with early endosomes isolated via the GFP-2xFYVE tag (GE Healthcare) at different times pre- and post-FGF stimulation.

tion (pY) and also interacted with ESyt2b (Fig. 6*D*). Further, the interactions of wild type and Y653,654E FGFR1 with ESyt2b were roughly proportional to their relative autophosphorylation levels and hence their relative catalytic activities, and both autophosphorylation and the ESyt interaction could be suppressed by the FGFR inhibitor SU5402 (Fig. 6*D*). We also generated an FGFR1 in which the Y653,654E mutation was combined with Y to F mutation of the other 5 phosphotyrosine sites (Y5F,653,654E) (Fig. 6*E*). This mutant receptor was able to recruit ESyt2b, though less efficiently than the wild type. However, in this case the SU5402 inhibitor unexpectedly caused an enhancement of the ESyt2b interaction. The Y653,654E phosphomimetic mutation of the activation loop clearly induces a structural change resembling that of the activated receptor (Fig. 6*D*). But, when combined with the five Y to F phosphosite mutations (Y5F,653,654E in Fig. 6*E*), it was quite possible that this structural change was enhanced by SU5402 binding to the ATP fold.

The data to this point strongly argued that no single phosphotyrosine or phosphotyrosine combination was required for the selective interaction of ESyt2b with the activated FGF receptor, and that even the activation loop tyrosines could be replaced by phosphomimetics. We concluded that either the activation loop phosphomimetics themselves were recognized by ESyt2b or the interaction did not require receptor phosphorylation at all and depended on a structural change.

ESyt2 Interaction Depends on an Active Receptor Conformation, not Its Catalytic Activity—The data from the phospho-site mutants suggested that phosphorylation did not play a direct role in the specificity of ESyt2 for the activated receptor, but that receptor activation was required. This suggested that ESyt2 might recognize a specific receptor conformation occurring on activation. FGFR1 activation is brought about by a displacement of the activation loop that allows access to the active site of the kinase domain (18). Further, FGFR1 autophosphorylation was shown to occur via an asymmetric inter-

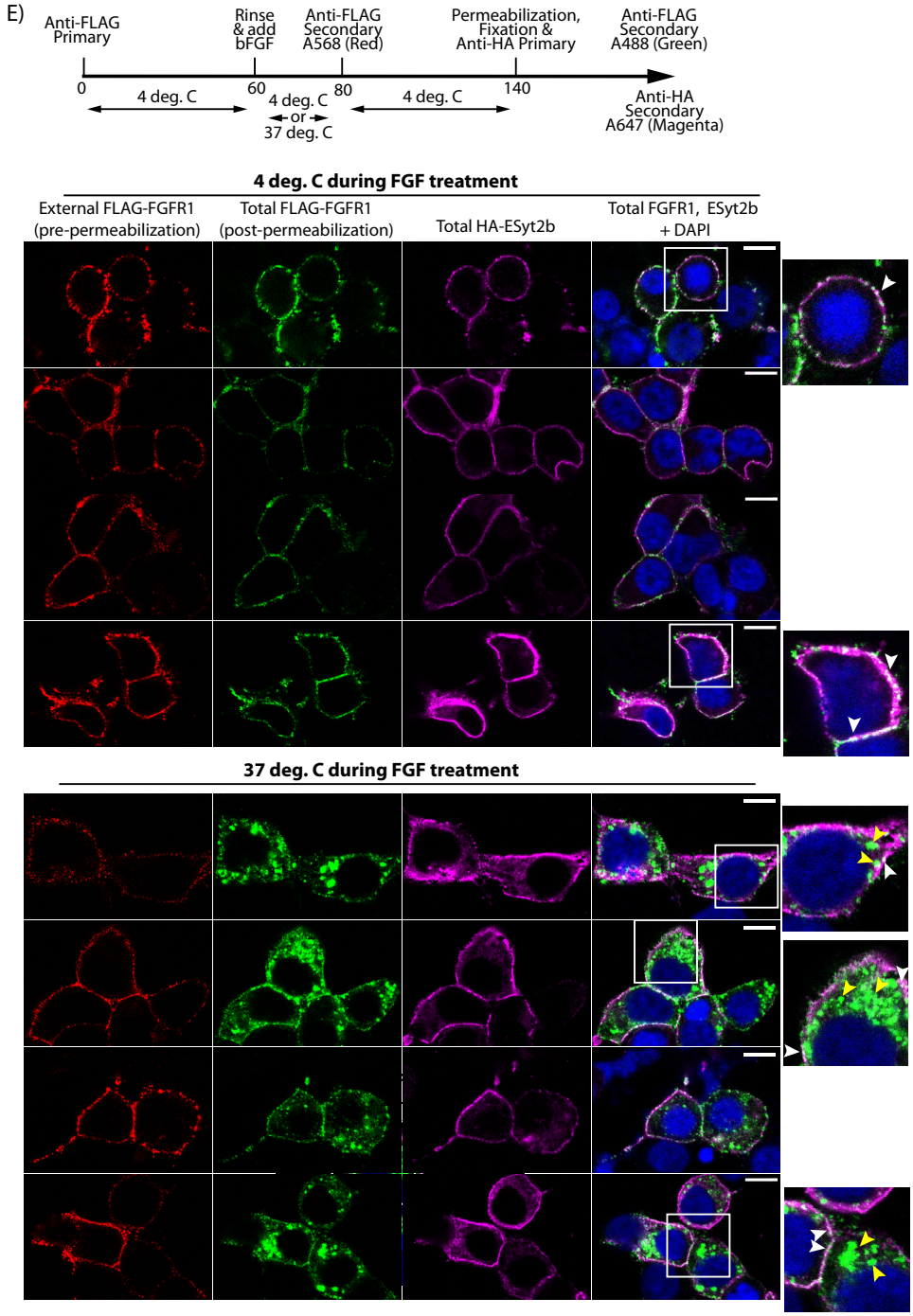

FIGURE 4—*Continued*

action between the kinase domains of adjacent receptors, one acting as enzyme and the other as substrate. Thus, receptor tyrosine phosphorylation actually occurs by a transphosphorylation event between the catalytic domains of a receptor dimer. Mutation of arginine aa 577 to glutamic acid (R577E) within the FGFR1 kinase domain was shown to prevent the asymmetric interaction required for this transphosphorylation event and, unexpectedly, to lock the activation loop in the open "active" conformation (19) (Fig. 7*A*). Thus, this mutation prevents the *in cell* interaction between catalytic domains of receptor dimers that permits their autophosphorylation, while at the same time locking the activation loop in the activated configuration. Indeed, the isolated FGFR1-R577E is catalytically active *in vitro* and able to phosphorylate a PLCγ substrate (19). We argued that if ESyt2b specifically recognized the conformation of the active FGFR1 it should interact with the R577E FGFR1 mutant regardless of its inability to autophosphorylate. ESyt2b did indeed interact with FGFR1-R577E, despite this mutant being clearly unable to autophosphorylate (Fig. 7*B*) and hence unable to recruit phospho-PLCγ (pY-PLCγ). As control we used the Y766F mutant that eliminates the phospho-site bound by PLCγ, but has no effect on receptor activation (20, 21).

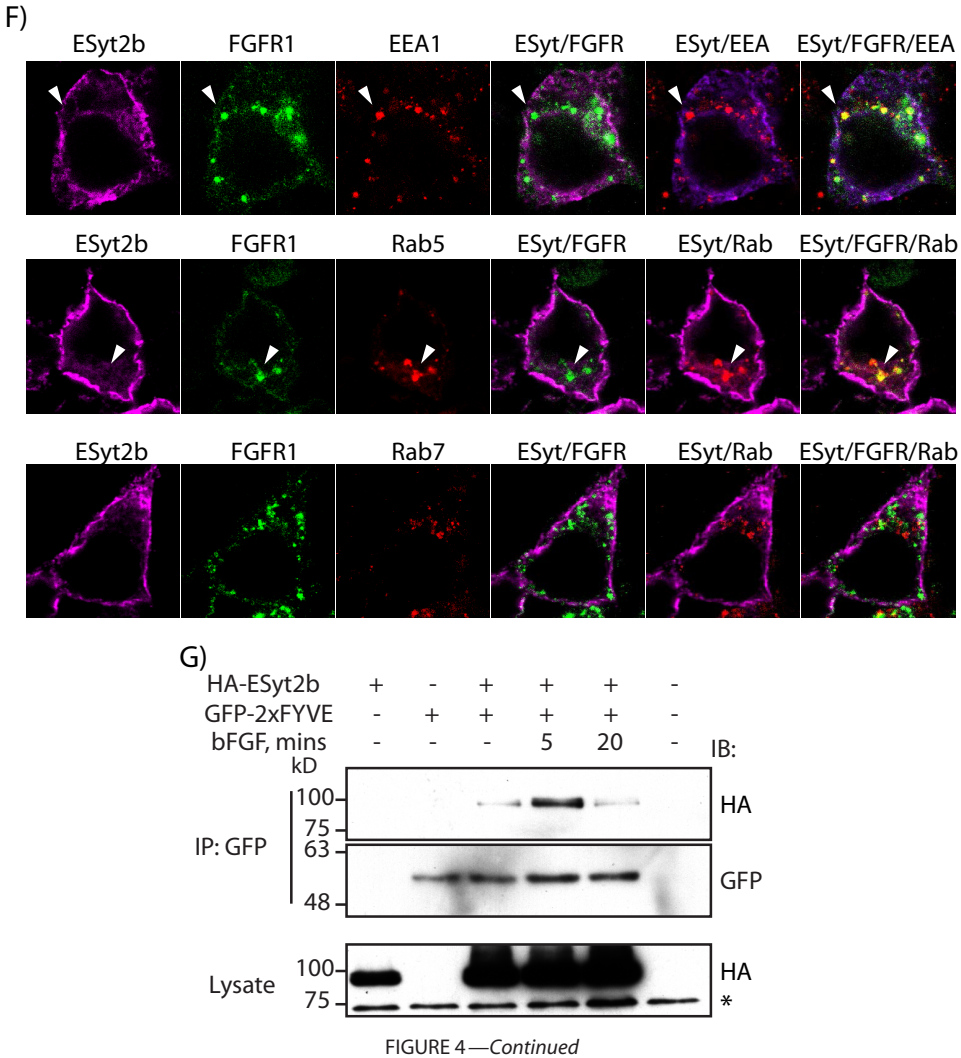

FIGURE 4—*Continued*

FRS2 is constitutively recruited to the receptor and hence for this reason was unlikely to be implicated in the ESyt2 interaction (22). However, to directly test this we also mutated the essential leucine 422 (L422A) within the FRS2 binding site on FGFR1, but found it had no effect on the ESyt2b interaction (Fig. 7*B*).

We further investigated the interaction of ESyt2b with the FGFR1-R577E mutant in comparison with the inhibited and activated states of the wild type receptor and the kinase dead ATP binding site mutant K514A (23). Both the wild type FGFR1 and the R577E inactive mutant interacted strongly with ESyt2b, while as should be expected, the K514A (KD) mutant did not (Fig. 7*C*). Interestingly, the inhibitor SU5402 strongly suppressed the interaction of ESyt2b with wild type FGFR1, but had no effect on the interaction of ESyt2b with the R577E mutant. Since this mutant binds ATP and SU5402, this further confirmed that the active receptor conformation and not its catalytic activity were sufficient for the ESyt2b interaction (24). Together these data show that ESyt2 specifically recognizes the open active conformation of FGFR1 independently of either catalytic activity or receptor autophosphorylation.

FGFR Truncation Reveals an Interaction with ESyt2b That Is Direct and Independent of Catalytic Activity—Because the data to this point indicated an ESyt2-FGFR1 interaction based solely on the recognition of the open receptor conformation, this suggested that displacement of the activation loop revealed an ESyt2 binding site that was otherwise hidden in the inactive receptor. Thus, we decided to ask if this surface would also be revealed in C-terminal receptor deletion mutants (Fig. 8*A*). Deletion of the C-terminal tail, leaving the kinase domain intact, as expected, had no effect on the ESyt2b interaction, as did deletion of the transmembrane domain proximal Nedd4-1 ubiquitinylation site (Δ6) shown to be required for receptor internalization (25) (Fig. 8*B*). Surprisingly, deletion of the lower C-terminal kinase lobe and the activation loop also had no effect on the ESyt2b interaction, but deletion to aa 475, to remove most of the N-terminal kinase lobe, eliminated the interaction. This supported the idea that ESyt2b recognized a binding site on FGFR1 contained within the N-terminal or upper C-terminal kinase lobes that was revealed on displacement of the activation loop during receptor activation. To further delineate the ESyt2b binding site, we created three more C-terminal deletion mutants of FGFR1. Partial deletion of the

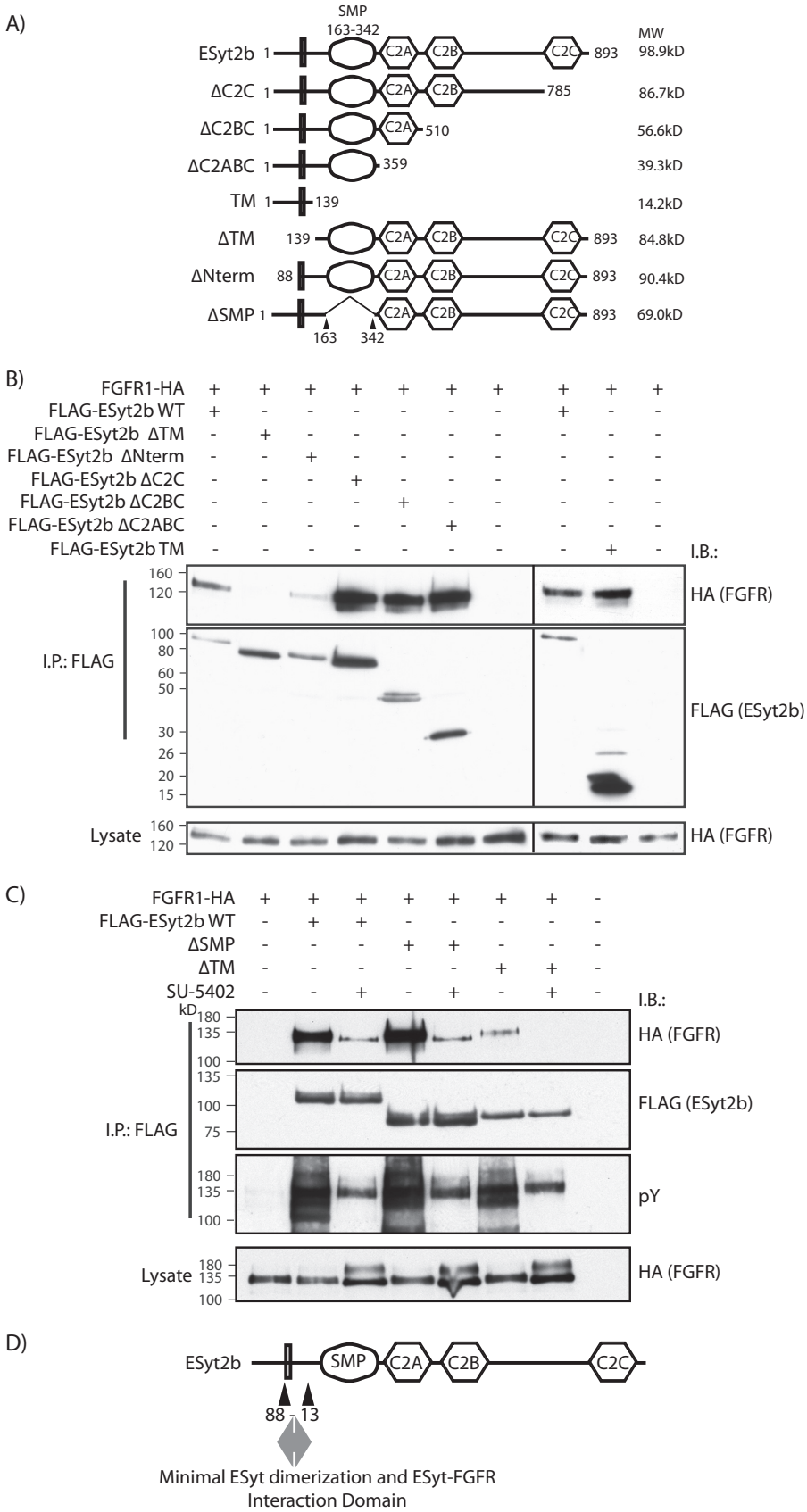

FIGURE 5. **ESyt2b interacts with FGFR1 via TM adjacent sequences.** *A*, diagrammatic structure of ESyt2b and corresponding deletion mutants. *B* and *C*, analysis of co-immunoprecipitation of C-terminally HA-tagged FGFR1 with N-terminally FLAG-tagged full-length ESyt2b and corresponding deletion mutants co-expressed in HEK293T cells. *D*, diagrammatic summary of the ESyt2b dimerization and FGFR1 interaction domain.

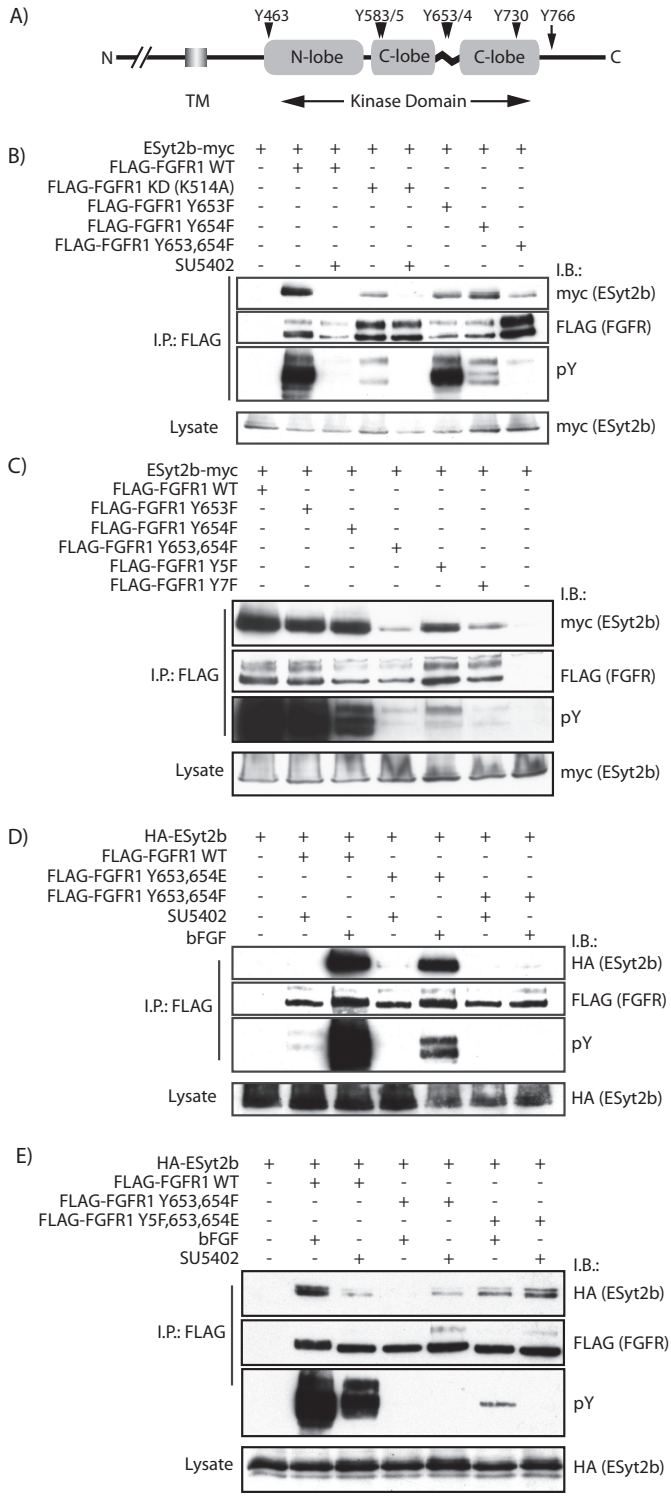

FIGURE 6. **The ESyt2b interaction with FGFR1 depends on receptor activation but not its autophosphorylation.** *A*, diagrammatic structure of the cytoplasmic region of FGFR1 showing the transmembrane sequence (*TM*), the N-terminal and upper and lower C-terminal lobes of the kinase domain, and the autophosphorylation sites. *B*, co-immunoprecipitation of C-terminally Myc-tagged ESyt2b with N-terminally FLAG-tagged wild type (WT), kinase dead (KD), and activation loop mutant (Y653 and/or 654F) FGFR1 forms co-expressed in HEK293T cells. In the cases of wild type and kinase dead forms of FGFR1, receptor inhibition with SU5402 demonstrates the high degree of selectivity of ESyt2b for the active form of the receptor. *C*, co-immunoprecipitation as in *B* of ESyt2b with combined FGFR1 autophosphorylation site mutants Y465,583,585,730,766F (Y5F) and Y465,583,585,653,654,730,766F (Y7F) in comparison with the WT receptor and the activation loop mutants Y653F, Y654F, and Y653,654F. *D*, co-immunoprecipitation of N-terminally HA-tagged ESyt2b with N-terminally FLAG tagged wild type FGFR1 (WT) and constitutively active Y653,654E and inactive Y653,654F activation loop mutants as in *B*, but after receptor activation with bFGF or inhibition with SU5402. *E*, co-immunoprecipitation as in *D* of ESyt2b with combined FGFR1 autophosphorylation site mutant Y465,583,585,730,766F in addition carrying the activation loop phosphomimetic mutations Y653,654E (Y5F,653,654E) in comparison with the WT receptor and the activation loop mutant Y653,654F. In *B–E*, receptor activation was monitored by its level of autophosphorylation (*pY*).

upper part of the C-terminal kinase lobe to aa 600, or indeed its full deletion to aa 550, had no effect on the interaction of ESyt2b with the receptor (Fig. 8*C*). However, deletion to aa 500, also removing half the N-terminal kinase lobe, did eliminate the ESyt2b binding site.

To this point the data, though very suggestive of a direct ESyt2/FGFR interaction, did not rule out the possibility that it required a bridging protein. To test this, we asked if the FGFR1 catalytic domain, expressed in *Escherichia coli* as a GST fusion protein, would bind ESyt2b translated *in vitro*. Multiple previous studies showed that the FGFR1 catalytic domain expressed in bacteria is already in the activated tyrosine-phosphorylated conformation, *e.g.* (26). G-Sepharose-immobilized wild type GST-FGFR1 (aa361–765) and the C-terminal truncation mutants (aa361–562 and -550) retained full-length ESyt2b, but did not retain the N-terminal truncation mutant ΔTM shown to strongly suppress FGFR1 binding in coimmunoprecipitation assays (see Fig. 5, *A* and *C*). Thus, the ESyt2b-FGFR1 interaction involves direct contacts between the N-terminal lobe of the FGFR1 catalytic domain and the N-terminal region of ESyt2b.

Together the data strongly suggest that the selectivity of ESyt2b for the active FGFR1 receptor depends on a binding site within the N-terminal kinase lobe of the receptor that is revealed when the activation loop is displaced to its position in the active receptor conformation. The probable structure of the N-terminal kinase lobe in the aa 550 deletion mutant is shown in Fig. 9*A*. Since we can fully delete the activation loop without affecting the ESyt2b-FGFR1 interaction, contact with the loop itself is clearly unnecessary for the interaction. However, within the context of the wild type FGFR1 the activation loop would prevent ESyt2 access to the underside of the N-terminal kinase lobe in its inactive configuration, but allow access in its active configuration (Fig. 9*B*). This in turn suggests that the site of the ESyt2 interaction lies proximal to or corresponds with the ATP-binding pocket.

Discussion

The interaction of ESyt2 with FGFR1 was previously shown to be dependent on receptor activation and to be required for a rapid phase of receptor internalization necessary for functional signaling via the ERK pathway during early *Xenopus* development and shown to be conserved in human (6). Here we have used the human system to investigate the molecular parameters of the ESyt-FGFR1 interaction in order to better understand its underlying specificity. However, ESyt2 is just one of the three member family of human Extended Synaptotagmins. These proteins were recently shown to be implicated in the formation of ER-PM junctions and in the Ca^{2+}-dependent regulation of these junctions (9–11). We provide evidence supporting the

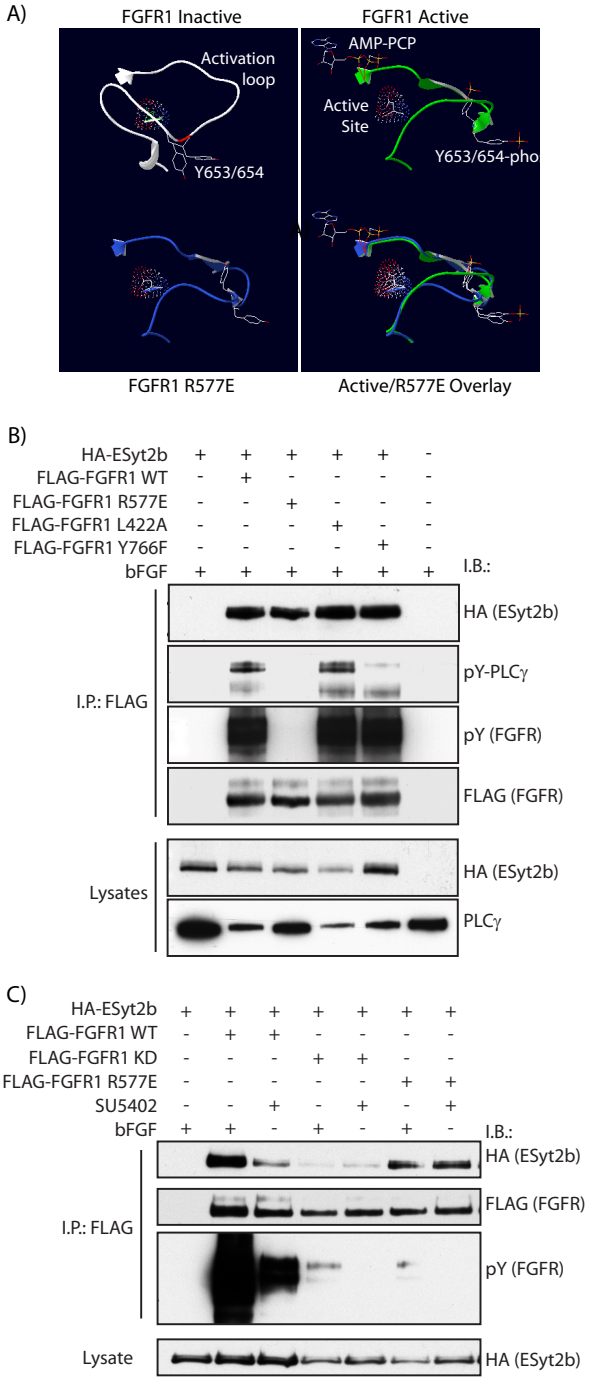

FIGURE 7. **ESyt2b recognizes the activated conformation of FGFR1 independently of catalytic activity.** *A*, path of the activation loops, respectively from *left* to *right*, *top* to *bottom*, for the inactive (*white*) (30) (PDB code: 3KY2), activated (Y653/654-phosphorylated, *green*) (18) (PDB code: 3QGI), R577E mutant (*blue*) (24) (PDB code: 3KXX), and overlaid "active" and R577E mutant FGFR1 configurations. The *dot surface* of the active site aspartic acid (*D623*) is indicated, as are tyrosine 653 and 654 (*Y653/654*) side chains and the position of the AMP-PCP non-hydrolyzable ATP analog within the inactive configuration. *B*, co-immunoprecipitation of N-terminally HA-tagged ESyt2b and N-terminally FLAG tagged wild type FGFR1 (*WT*), or the corresponding R577E, L422A, and Y766F receptor mutants after co-expression of ESyt2b and receptors in HEK293T cells and receptor activation with bFGF. Endogenous PLCγ and phospho-PLCγ (*pY-PLCγ*) were monitored using specific antibodies. *C*, co-immunoprecipitation of N-terminally HA-tagged ESyt2b with N-terminally FLAG-tagged wild type FGFR1 (WT), or the corresponding kinase-dead K514A (KD) and R577E receptor mutants as in *B*, but after receptor activation with bFGF or inhibition with SU5402. In *B* and *C*, receptor activation levels were monitored by the level of receptor tyrosine autophosphorylation (*pY*).

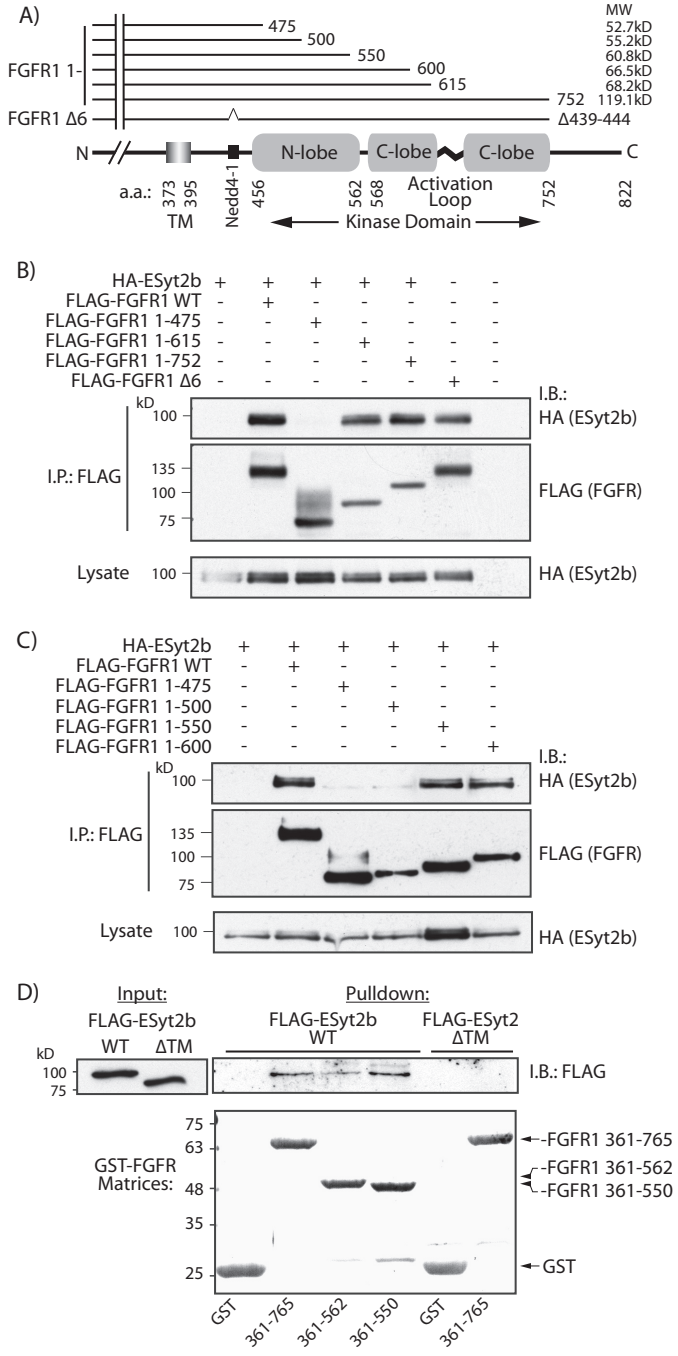

FIGURE 8. **C-terminal deletions of FGFR1 reveal that ESyt2b interacts with the N-terminal lobe of the receptor kinase domain both in coimmunoprecipitation and *in vitro* pulldown experiments.** *A*, extent of deletion mutants of FGFR1 as compared with the organization of the cytoplasmic domain of the receptor. *B* and *C*, co-immunoprecipitation of N-terminally HA-tagged ESyt2b with N-terminally FLAG-tagged full-length (WT) FGFR1 and corresponding receptor deletion mutants. The Nedd4-1 ubiquitinylation site aa439–444 deletion mutant (FGFR1 Δ6) (25), independently generated in our laboratory, was included in *B* to show that this modification did not play a part in the ESyt2b interaction. Despite this, other analyses confirmed the published role of the Nedd4-1 site in receptor internalization (data not shown). *D*, pull-down of *in vitro* translated FLAG-ESyt2b and ESyt2b ΔTM (see Fig. 5*A*) by bacterially expressed and immobilized GST-fused FGFR1 catalytic domain fragments aa361–752, aa361–562, and aa361–550 and GST alone. *Upper panels* show the input and pull-down *in vitro* translated ESyt2b revealed by anti-FLAG immunoblotting and the *lower panel*, the same membrane stained with Ponceau Red to reveal the corresponding immobilized GST-fusion proteins. The experiment was also performed using [S^{35}]methionine-labeled ESyt2b proteins and gave the same interaction profiles.

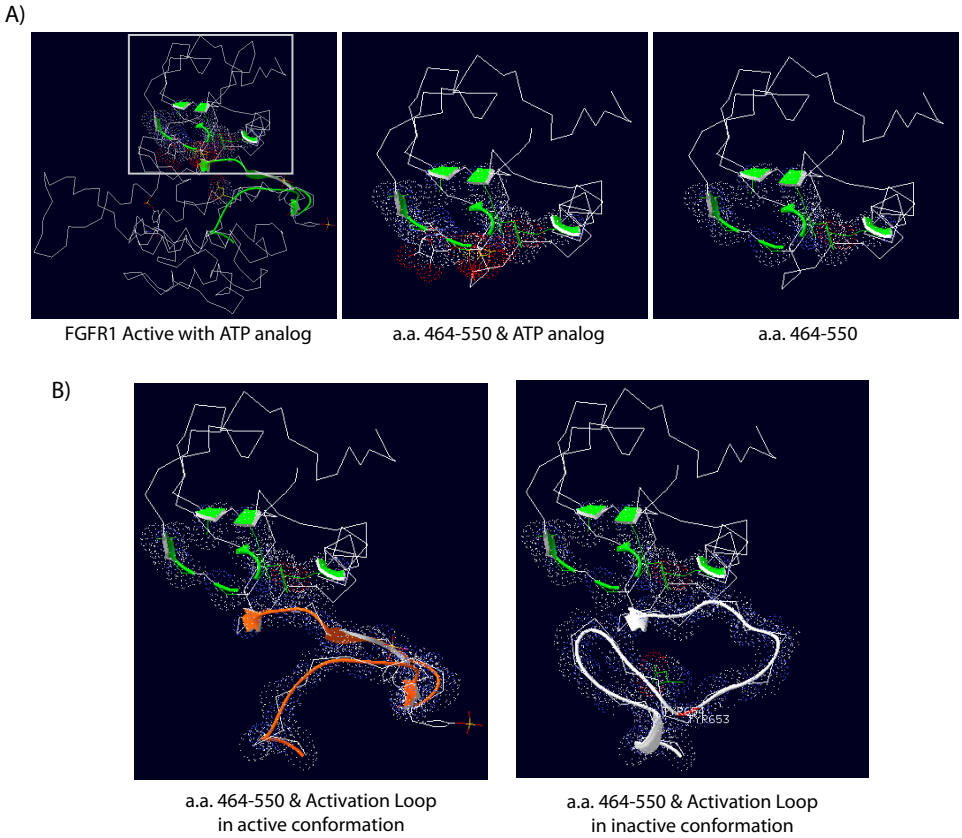

FIGURE 9. **The conformation of the activation loop may control access to the ESyt2b binding site.** *A*, *left panel*: the structure of the activated FGFR1 kinase domain with the ATP analog AMP-PCP bound, the N-terminal kinase lobe is shown boxed. *Right panels*: the probable structure of aa464–550 in the corresponding C-terminal FGFR1 deletion mutant aa1–550, in the presence and absence of the ATP analog. *B*, probable structure of the N-terminal kinase lobe in the C-terminal FGFR1 deletion mutant aa1–550 superimposed on the *left* with the active and on the *right* the inactive conformations of the activation loop. The N-terminal lobes in *A* and *B* are taken from the activated catalytic domain FGFR1 structure (18) (PDB code: 3QGI), while the superimposed activation loop structures in *B* are taken from the activated (*red*) (18) (PDB code: 3QGI) and inactive (*white*) (30) (PDB ID: 3KY2) catalytic domain structures. Images were generated using Swiss-PdbViewer.

observations (10, 11) that the ESyts are not integral PM proteins, but rather are inserted into the ER membrane. We also show that, in the case of ESyt2, this function is an intimate property of the putative transmembrane domain, since its replacement by the transmembrane domain of Syt1 redirects ESyt2 to the PM. We further show that all three ESyts hetero- and homodimerize to some degree, though ESyt1 may prefer to heterodimerize with ESyt2 rather than with ESyt3. Analysis of ESyt2b deletion mutants showed that neither the C2 domains nor the SMP domain are essential for its homodimerization *in vivo*. This suggests that the dimerization via the SMP domain observed in the ESyt2b crystal structure is not essential for its dimerization *in vivo* (15).

We show that ESyt2 (both a and b splice variants) and ESyt3, but not ESyt1, selectively interact *in vivo* with the activated form of FGFR1. Interaction of ESyt2b with FGFR1 depends strongly, if not exclusively, on the TM and immediately adjacent sequences of ESyt2 (aa 88 to 138). This region is common to ESyt2a and 2b and shows 45% identity/71% similarity with the equivalent region of ESyt3 and 41% identity/61% similarity with the equivalent of ESyt1. Thus, the lack of an interaction of ESyt1 with FGFR may in part be due to the lower homology with ESyt2/3 or to its predominant localization to cytoplasmic ER membranes (10, 11), or both.

We further investigated the factors that determine the selective interaction of ESyt2b with activated FGFR1. We found that while receptor activation is a prerequisite for the interaction, none of the receptor autophosphorylation events were required. Indeed, even the activation loop phospho-sites Tyr-653 and Tyr-654 of FGFR1 could be replaced by phospho-mimics (Y653/654E) without affecting either the interaction with ESyt2 or its specificity. Combining these mutations with Tyr to Phe mutation of the five other phosphotyrosine sites (Y5F,653,654F, Fig. 6*E*) confirmed that none of the sites were directly involved in the interaction. However, it was clear that such extensive mutation of the receptor could have important structural effects, potentially explaining why ESyt2 binding was now enhanced rather than suppressed by the ATP analog inhibitor SU5402 (Fig. 6*E*). Though this was an unexpected result, it did serve to finally confirm that the catalytic activity of the receptor was not required for interaction with ESyt2, and suggested a role for receptor conformation. Later data in fact showed that ESyt2 binds a surface in the upper kinase lobe of the receptor close to the ATP fold, providing a potential explanation for the contradictory effect of SU5402 in the context of the Y5F,653,654F FGFR1 mutant. However, the interaction of ESyt2 with the R577E FGFR1 mutant confirmed that the ESyt2-FGFR1 interaction was indeed dependent on precise receptor conforma-

tion, not activity. The R577E mutation renders FGFR1 catalytically inactive *in vivo*. In contrast, atomic structure determination showed that this mutation locked the activation loop in the open, active configuration, but otherwise has little effect on kinase domain structure (Fig. 7*A*) (19). Thus, the ability of ESyt2 to efficiently interact with FGFR1-R577E strongly argued that the interaction was based solely on activation loop conformation and not catalytic activity. This finding suggested that ESyt2 recognized a surface on the FGFR1 catalytic domain that was revealed by displacement of the activation loop. Receptor deletion mapping confirmed this was the case and showed that the interaction site between ESyt2b and FGFR1 lay within the N-terminal kinase lobe of the receptor, probably close to the ATP binding fold. We further demonstrated *in vitro* that this interaction was direct. Together, the data strongly suggest that the conformation of the receptor activation loop defines access of ESyt2 to the lower surface of the N-terminal FGFR1 kinase lobe including the ATP-binding pocket (Fig. 9). This then explains the high degree of selectivity of ESyt2 and probably ESyt3 for the active form of the FGF receptor.

Our previous data showed that ESyt2 was required in very early *Xenopus* embryos for functional FGF signaling via the ERK but not the PI3-kinase pathways. The data further demonstrated a function of ESyt2 in a rapid phase of receptor endocytosis in these embryos. Recent data showing that ESyt2 and 3 localize to ER-PM junctions and may act in concert with other junctioning proteins (9) suggests that this function may be only one part of a more complex pathway regulating FGF signaling that involves the regulation of Ca^{2+} and phosphatidylinositol 4,5-bisphosphate (PIP2) levels (10). FGF signaling directly activates PLCγ, *e.g.* see Fig. 7*B*, and hence stimulates the cleavage of PIP2 and the release of Ca^{2+} into the cytosol (27). This release of Ca^{2+} was shown to stimulate ESyt1 recruitment to, or the tightening of, ER-PM junctions and the replenishment of PIP2 on the PM (10). Such a feedback mechanism would effectively prolong or enhance signaling via the PLCγ pathway and hence have an important modulating influence on intracellular signaling. Consistent with this, parallel mass spectrometric studies have shown that the interaction of ESyt2 with ESyt1 is dependent on FGFR activation.[3] Ca^{2+} has also been shown in other systems to modulate clathrin-dependent endocytosis (28, 29). Thus, the response of the ESyts to Ca^{2+} release may explain their ability to modulate growth factor signaling in *Xenopus* by controlling the rate of endocytosis (6). Further studies of the ESyts is certain to generate insight into the mechanisms that underly the cell-specific outcomes of growth factor signaling.

Acknowledgments—We thank Drs. J. Wesche and E. M. Haugsten for providing a wild type human FGFR1 construct, and the Sequencing and Genotyping Service of the Quebec University Hospital Research Centre.

[3] Proteins contained in FLAG immunoprecipitates from FGF stimulated or unstimulated HEK293T cells expressing triple FLAG-tagged Human ESyt2b were determined by mass spectrometry in comparison with controls from unexpressing cells, F. Guillou, unpublished data.

References

1. Moghadam, P. K., and Jackson, M. B. (2013) The functional significance of synaptotagmin diversity in neuroendocrine secretion. *Front. Endocrinol.* **4,** 124
2. Morris, N. J., Ross, S. A., Neveu, J. M., Lane, W. S., and Lienhard, G. E. (1999) Cloning and preliminary characterization of a 121 kDa protein with multiple predicted C2 domains. *Biochim. Biophys. Acta* **1431,** 525–530
3. Min, S. W., Chang, W. P., and Südhof, T. C. (2007) E-Syts, a family of membranous Ca2+-sensor proteins with multiple C2 domains. *Proc. Natl. Acad. Sci. U.S.A.* **104,** 3823–3828
4. Lee, I., and Hong, W. (2006) Diverse membrane-associated proteins contain a novel SMP domain. *Faseb J.* **20,** 202–206
5. Herdman, C., Tremblay, M. G., Mishra, P. K., and Moss, T. (2014) Loss of Extended Synaptotagmins ESyt2 and ESyt3 does not affect mouse development or viability, but *in vitro* cell migration and survival under stress are affected. *Cell Cycle* **13,** 2616–2625
6. Jean, S., Mikryukov, A., Tremblay, M. G., Baril, J., Guillou, F., Bellenfant, S., and Moss, T. (2010) Extended-synaptotagmin-2 mediates FGF receptor endocytosis and ERK activation *in vivo*. *Dev. Cell* **19,** 426–439
7. Creutz, C. E., Snyder, S. L., and Schulz, T. A. (2004) Characterization of the yeast tricalbins: membrane-bound multi-C2-domain proteins that form complexes involved in membrane trafficking. *Cell Mol. Life Sci.* **61,** 1208–1220
8. Jean, S., Tremblay, M. G., Herdman, C., Guillou, F., and Moss, T. (2012) The endocytic adapter E-Syt2 recruits the p21 GTPase activated kinase PAK1 to mediate actin dynamics and FGF signalling. *Biol. Open* **1,** 731–738
9. Manford, A. G., Stefan, C. J., Yuan, H. L., Macgurn, J. A., and Emr, S. D. (2012) ER-to-plasma membrane tethering proteins regulate cell signaling and ER morphology. *Dev. Cell* **23,** 1129–1140
10. Chang, C. L., Hsieh, T. S., Yang, T. T., Rothberg, K. G., Azizoglu, D. B., Volk, E., Liao, J. C., and Liou, J. (2013) Feedback regulation of receptor-induced ca(2+) signaling mediated by e-syt1 and nir2 at endoplasmic reticulum-plasma membrane junctions. *Cell Rep.* **5,** 813–825
11. Giordano, F., Saheki, Y., Idevall-Hagren, O., Colombo, S. F., Pirruccello, M., Milosevic, I., Gracheva, E. O., Bagriantsev, S. N., Borgese, N., and De Camilli, P. (2013) PI(4,5)P(2)-dependent and Ca(2+)-regulated ER-PM interactions mediated by the extended synaptotagmins. *Cell* **153,** 1494–1509
12. Reed, S. E., Staley, E. M., Mayginnes, J. P., Pintel, D. J., and Tullis, G. E. (2006) Transfection of mammalian cells using linear polyethylenimine is a simple and effective means of producing recombinant adeno-associated virus vectors. *J. Virol. Methods* **138,** 85–98
13. Boussif, O., Lezoualc'h, F., Zanta, M. A., Mergny, M. D., Scherman, D., Demeneix, B., and Behr, J. P. (1995) A versatile vector for gene and oligonucleotide transfer into cells in culture and in vivo: polyethylenimine. *Proc. Natl. Acad. Sci. U.S.A.* **92,** 7297–7301
14. Scott, R. P., Eketjäll, S., Aineskog, H., and Ibáñez, C. F. (2005) Distinct turnover of alternatively spliced isoforms of the RET kinase receptor mediated by differential recruitment of the Cbl ubiquitin ligase. *J. Biol. Chem.* **280,** 13442–13449
15. Schauder, C. M., Wu, X., Saheki, Y., Narayanaswamy, P., Torta, F., Wenk, M. R., De Camilli, P., and Reinisch, K. M. (2014) Structure of a lipid-bound extended synaptotagmin indicates a role in lipid transfer. *Nature* **510,** 552–555
16. Seet, B. T., Dikic, I., Zhou, M. M., and Pawson, T. (2006) Reading protein modifications with interaction domains. *Nat. Rev. Mol. Cell Biol.* **7,** 473–483
17. Furdui, C. M., Lew, E. D., Schlessinger, J., and Anderson, K. S. (2006) Autophosphorylation of FGFR1 kinase is mediated by a sequential and precisely ordered reaction. *Mol. Cell* **21,** 711–717
18. Bae, J. H., Lew, E. D., Yuzawa, S., Tomé, F., Lax, I., and Schlessinger, J. (2009) The selectivity of receptor tyrosine kinase signaling is controlled by a secondary SH2 domain binding site. *Cell* **138,** 514–524
19. Bae, J. H., and Schlessinger, J. (2010) Asymmetric tyrosine kinase arrangements in activation or autophosphorylation of receptor tyrosine kinases. *Mol. Cells* **29,** 443–448

20. Mohammadi, M., Dionne, C. A., Li, W., Li, N., Spivak, T., Honegger, A. M., Jaye, M., and Schlessinger, J. (1992) Point mutation in FGF receptor eliminates phosphatidylinositol hydrolysis without affecting mitogenesis. *Nature* **358,** 681–684
21. Peters, K. G., Marie, J., Wilson, E., Ives, H. E., Escobedo, J., Del Rosario, M., Mirda, D., and Williams, L. T. (1992) Point mutation of an FGF receptor abolishes phosphatidylinositol turnover and Ca2+ flux but not mitogenesis. *Nature* **358,** 678–681
22. Ong, S. H., Guy, G. R., Hadari, Y. R., Laks, S., Gotoh, N., Schlessinger, J., and Lax, I. (2000) FRS2 proteins recruit intracellular signaling pathways by binding to diverse targets on fibroblast growth factor and nerve growth factor receptors. *Mol. Cell Biol.* **20,** 979–989
23. Bellot, F., Crumley, G., Kaplow, J. M., Schlessinger, J., Jaye, M., and Dionne, C. A. (1991) Ligand-induced transphosphorylation between different FGF receptors. *EMBO J.* **10,** 2849–2854
24. Bae, J. H., Boggon, T. J., Tomé, F., Mandiyan, V., Lax, I., and Schlessinger, J. (2010) Asymmetric receptor contact is required for tyrosine autophosphorylation of fibroblast growth factor receptor in living cells. *Proc. Natl. Acad. Sci. U.S.A.* **107,** 2866–2871
25. Persaud, A., Alberts, P., Hayes, M., Guettler, S., Clarke, I., Sicheri, F., Dirks, P., Ciruna, B., and Rotin, D. (2011) Nedd4–1 binds and ubiquitylates activated FGFR1 to control its endocytosis and function. *EMBO J.* **30,** 3259–3273
26. Mohammadi, M., Honegger, A. M., Rotin, D., Fischer, R., Bellot, F., Li, W., Dionne, C. A., Jaye, M., Rubinstein, M., and Schlessinger, J. (1991) A tyrosine-phosphorylated carboxy-terminal peptide of the fibroblast growth factor receptor (Flg) is a binding site for the SH2 domain of phospholipase C-γ1. *Mol. Cell. Biol.* **11,** 5068–5078
27. Thisse, B., and Thisse, C. (2005) Functions and regulations of fibroblast growth factor signaling during embryonic development. *Dev. Biol.* **287,** 390–402
28. Yamashita, T. (2012) Ca2+-dependent regulation of synaptic vesicle endocytosis. *Neurosci. Res.* **73,** 1–7
29. Andersen, C. B., and Moestrup, S. K. (2014) How calcium makes endocytic receptors attractive. *Trends Biochem. Sci.* **39,** 82–90
30. Mohammadi, M., Schlessinger, J., and Hubbard, S. R. (1996) Structure of the FGF receptor tyrosine kinase domain reveals a novel autoinhibitory mechanism. *Cell* **86,** 577–587
31. Guex, N., and Peitsch, M. C. (1997) SWISS-MODEL and the Swiss-PdbViewer: an environment for comparative protein modeling. *Electrophoresis* **18,** 2714–2723